

1 **A GCM-based analysis of circulation controls on $\delta^{18}\text{O}$ in the southwest**

2 **Yukon, Canada: implications for climate reconstructions in the region**

3 **Robert D. Field¹, G.W.K. Moore¹, Gerald Holdsworth², Gavin A. Schmidt³**

4 **¹. Department of Physics, University of Toronto, Toronto, Canada**

5 **². Arctic Institute of North America, University of Calgary, Calgary, Canada**

6 **³. NASA Goddard Institute for Space Studies, New York, USA**

7

8 **Running title:** Controls on $\delta^{18}\text{O}$ in the SW Yukon

9 **Abstract**

10 To improve our understanding of paleoclimatic records in the southwest Yukon, we
11 examined controls on precipitation $\delta^{18}\text{O}$ using an isotopically-equipped atmospheric
12 general circulation model (GCM). Our results show that, particularly during the cool-
13 season, elevated $\delta^{18}\text{O}$ is associated with a deeper Aleutian Low and stronger southerly
14 moisture flow, while lower $\delta^{18}\text{O}$ is associated with the opposite meteorological
15 conditions. These results suggest that the large mid-19th century shift towards lower $\delta^{18}\text{O}$
16 values seen in paleoclimate records from the region was associated with a shift towards a
17 weaker Aleutian Low. While in disagreement with a previous interpretation of this shift,
18 it is consistent with records of glacial advance and tree-ring growth during the same
19 period, and observational studies of Aleutian Low controls on temperature and
20 precipitation in the region.

21 **1. Introduction**

22 Stable water isotopes preserved in ice cores and other paleoclimatic sources are an
23 important source of climate information prior to the instrumental record [Dansgaard,
24 1964; Jones and Mann, 2003]. Our interest is in better understanding isotopic records
25 from the southwest Yukon region, and any information they might contain about past
26 atmospheric circulation. In particular, a significant drop in mean $\delta^{18}\text{O}$ occurred during the
27 middle of the 19th century in two separate ice cores extracted from Mt. Logan in the
28 southwest Yukon, just to the east of the Gulf of Alaska [Holdsworth et al., 1992; Fisher et
29 al., 2004], and in sediment carbonate $\delta^{18}\text{O}$ recovered from a lake also in the SW Yukon
30 [Anderson et al., 2005]. The $\delta^{18}\text{O}$ record from the Northwest Col at 5340m asl shows this
31 shift as a 2-3‰ depletion during the late 1840s (Figure 1). Using an analytical model,
32 Fisher et al. [2004] interpreted this shift as being caused by a stronger Aleutian Low
33 (AL), which brought moisture originating from more distant, southerly sources, and
34 owing to this greater distance, enhanced isotopic depletion.

35 It is difficult to reconcile this interpretation of the $\delta^{18}\text{O}$ shift, however, with climate
36 reconstructions in the region during the 19th century. D'Arrigo et al. [2005], for example,
37 used tree-ring samples ringing the North Pacific to reconstruct the strength of the AL
38 since the 17th century, identifying a significant mid-19th century weakening of the AL, in
39 disagreement with the interpretation of Fisher et al. In this study we used an isotopically-
40 equipped general circulation model (GCM) to better understand controls on the $\delta^{18}\text{O}$
41 composition of precipitation in the SW Yukon, in order better interpret isotopic archives
42 in the region.

43 **2. Data and methods**

44 Since their development in the 1980s [Joussaume et al., 1984], isotopically-equipped
45 GCMs have been an important tool in identifying controls on precipitation $\delta^{18}\text{O}$. In these
46 GCMs, the fractionation between heavy and light isotopes is modeled through all stages
47 of the hydrological cycle. Unlike the GCM, steady-state models such as that used in
48 Fisher et al. [2004] rely upon a number of empirical factors, such as the balance between
49 zonal and meridional transport, being prescribed in order to produce a realistic present-
50 day climatology. Isotopically-equipped GCMs have been used to better understand
51 controls on $\delta^{18}\text{O}$ over the polar ice sheets and other major ice-coring sites [eg. Werner
52 and Heimann, 2002; Vuille et al., 2003].

53 In this paper, we used the GISS ModelE GCM [Schmidt et al., 2005], run at a $4^\circ \times 5^\circ$
54 horizontal resolution with 20 vertical levels for 45 years starting in 1954, forced with
55 interannually-varying sea-surface temperature and sea-ice fields from the HadISST 1.1
56 dataset [Rayner et al., 2003]. The choice of simulation period was arbitrary and, as such,
57 ours is an analogue study, where we assume that any immediate meteorological controls
58 on precipitation $\delta^{18}\text{O}$ are persistent across time.

59 Correlation maps were created between precipitation $\delta^{18}\text{O}$ over the SW Yukon and
60 sea-level pressure and moisture flux in the spatial domain. Moisture flux between 974
61 hPa and 909 hPa was computed as a vertically-integrated quantity following Peixoto and
62 Oort [1992]. As in Werner and Heimann [2002], we considered the $\delta^{18}\text{O}$ values spanning
63 several grid points (58 to 64N, 142 to 132W) rather than a single grid point. In
64 calculating $\delta^{18}\text{O}$ averages, monthly values were weighted by precipitation amount, and
65 we allowed for different seasonal controls by also constructing correlation maps

66 separately for the warm season (March through August) and cool season (September
67 through February). We also substituted surface temperature and precipitation amount for
68 precipitation $\delta^{18}\text{O}$ over the SW Yukon, to understand circulation controls on basic
69 climate parameters.

70 Finally, we constructed correlation maps between mid-tropospheric moisture
71 circulation and vapor $\delta^{18}\text{O}$ over the SW Yukon analysis region. Identifying controls on
72 vapor $\delta^{18}\text{O}$ provided an additional check on controls on the moisture reservoir above the
73 ice core site, the topography around which is only very coarsely resolved by the GCM.
74 and which does not allow the model to capture the altitude-driven depletion at the ice
75 core drill sites, Moisture-weighted, mean vapor $\delta^{18}\text{O}$ was calculated between 760 and 470
76 hPa over the analysis region, and correlated against the fields of moisture circulation
77 between 760 and 470 hPa and geopotential height at 630 hPa.

78 **3. Results**

79 Observed $\delta^{18}\text{O}$ values at GNIP stations in the region were generally well-simulated
80 by the GCM (Table 1). At Barrow on Alaska's North Slopes, modeled DJF and JJA $\delta^{18}\text{O}$
81 means of -22.7‰ and -15.8‰, respectively, were close to the observed means of -21.1‰
82 and -14.7‰. Modeled and observed values were also in good agreement for Bethel, in the
83 southwest corner of Alaska. The model did not capture the cold season depletion in
84 Whitehorse, or at the plateau of the two Logan drill sites (~ -32 ‰), where the sharp
85 orographic rainout cannot be captured by the low topographic resolution of the model
86 Further inland at Yellowknife in the NWT, however, the modeled DJF and JJA $\delta^{18}\text{O}$
87 means of -24.2 ‰ and -14.9 ‰ are in good agreement with the observed means of -

88 25.1‰ and -16.8‰. We emphasize that any controls identified reflect those over the SW
89 Yukon in general, and not for a specific proxy site.

90 Annually, there is some evidence of control on SW Yukon precipitation $\delta^{18}\text{O}$ by
91 atmospheric circulation in the North Pacific (Figure 2a), with an indication of less
92 depleted $\delta^{18}\text{O}$ being associated with southerly flow and a negative SLP correlation over
93 southwestern Alaska. There is stronger evidence of control over vapor $\delta^{18}\text{O}$ (Figure 2b),
94 with an additional center of positive 630 hPa geopotential height correlation east of the
95 analysis region, which is associated with anticyclonic circulation and, given its position,
96 southeasterly flow into the analysis region. The strongest annual controls are on
97 precipitation amount (Figure 2c) and temperature (Figure 2d). The negative correlation
98 pattern centered over the Gulf of Alaska associates a deeper Aleutian Low with enhanced
99 precipitation and warmer temperatures over the analysis region. During the warm season
100 (Figure S1), the circulation controls are generally weaker than for the annually-averaged
101 cases.

102 The circulation controls on precipitation $\delta^{18}\text{O}$ over the SW Yukon are much stronger
103 during the cool season (Figure 3a), with a strong association between less depleted
104 precipitation $\delta^{18}\text{O}$ and more southerly moisture flux around a deeper Aleutian Low. The
105 same relationship appears for vapor $\delta^{18}\text{O}$ in the mid-troposphere (Figure 3b), but as part
106 of a tripole, with a positive, anti-cyclonic center over western North America and a
107 negative, cyclonic centre over the eastern US. To varying degrees across seasons, tropical
108 Pacific signatures appear in the SLP correlations, with less depleted $\delta^{18}\text{O}$, and wetter and
109 warmer conditions over the SW Yukon, associated with positive pressure anomalies over
110 the western Pacific.

111 We note that similar cool-season controls on $\delta^{18}\text{O}$ were identified using composite
112 maps (not shown). These composites were associated with a $\sim 1.5\text{‰}$ difference in low and
113 high $\delta^{18}\text{O}$ years over the SW Yukon, slightly less than the observed mid-19th century shift
114 in the ice core.

115 **4. Discussion**

116 Our results indicate that less depleted $\delta^{18}\text{O}$ over the SW Yukon is associated with
117 southerly moisture flux into the region. This moisture flux, in turn, is associated with
118 enhanced cyclonic circulation around a deeper Aleutian Low. In the mid-troposphere,
119 our results indicate the presence of the tripole-like control on vapor $\delta^{18}\text{O}$ (Figure 3b) as
120 well as a surface feature related to the AL (Figure 3a). These features are similar to the
121 Pacific-North America (PNA) teleconnection identified by Wallace and Gutzler [1981]
122 whose surface expression is the AL. The positive SLP correlations across the western
123 equatorial Pacific, although less robust across seasons, are indicative of warm ENSO
124 conditions. This relationship between warm ENSO, a deeper AL and positive PNA is
125 consistent with observational studies [Trenberth and Hurrell, 1994] and controls on Mt.
126 Logan snow accumulation [Moore et al., 2002].

127 Seasonality is important in controlling $\delta^{18}\text{O}$, due mainly to persistent features such as
128 AL often being wintertime-only phenomena [Trenberth and Hurrell, 1994]. The effects of
129 seasonality on $\delta^{18}\text{O}$ controls has also been observed for Greenland, where a strong NAO
130 signature was seen in winter months, but only weakly during summer months [Rogers et
131 al., 1998], due to the relative summer weakness of North Atlantic features such as the
132 Icelandic Low. Stronger wintertime circulation controls were also observed in the Mt.
133 Logan snow accumulation [Moore et al., 2002; Rupper et al., 2004].

134 The results that we have presented have important implications for the analysis of ice
135 core $\delta^{18}\text{O}$, which, in all but a few studies, are conducted using annually-averaged data. In
136 the case of the Mt. Logan ice cores, the inclusion of weakly-controlled summer values in
137 taking an annual average could mute any strong controls present during the winter. Use
138 of a winter-only $\delta^{18}\text{O}$ record from the ice core may lead to more consistent relationships
139 between the isotopic records and paleoclimate reconstructions from other sources such as
140 AL strength from tree-rings, and enhance reconstructions of winter-only teleconnections
141 such as the PNA using the ice core record. This will be done for the Mt. Logan ice core in
142 a future study.

143 In interpreting these circulation controls in a paleoclimatic context, we therefore
144 found no evidence that the 1840s to 1850s shift towards more depleted $\delta^{18}\text{O}$ values
145 observed at Mt. Logan and Jellybean Lake was associated with a strengthening of the
146 Aleutian Low. Rather, our results suggest that the dominant effect of a deepened AL is to
147 reduce isotopic depletion during transport to the SW Yukon. Physically, the less-depleted
148 precipitation $\delta^{18}\text{O}$ in the SW Yukon under these conditions could be attributed to several
149 processes, namely: enhanced evaporative recharge or reduced rainout along a more
150 southern path, increased mixing with less isotopically-depleted air masses under eddy-
151 dominated moisture transport [Alley and Cuffey, 2001], or weaker isotopic fractionation
152 under warmer conditions. Although there is likely some entrainment of sub-tropical
153 moisture, the observational analysis of Zhu et al. [2007], for example, showed no
154 cyclones originating south of 30N; the Fisher et al. [2004] association between stronger
155 AL with more depleted $\delta^{18}\text{O}$ is possibly due to an unrealistically large contribution of
156 tropical moisture.

157 There is also the possibility that the mid-19th century shift can be explained not by a
158 change in the AL strength, but rather by a change in precipitation seasonality. While we
159 can not fully exclude this, we do note that the controls identified here are consistent with
160 the north Pacific circulation reconstruction of D'Arrigo et al. [2005], and other types of
161 evidence during the mid 19th century. Observational analyses during the instrumental
162 period have shown that a stronger AL is also associated with warmer temperatures over
163 Alaska [Mock et al., 1998] and northwestern North America in general [Trenberth and
164 Hurrell, 1994], which was observed consistently in controls on temperature and
165 precipitation inferred from our GCM analysis. If a mid-19th-century deepening of the
166 Aleutian Low had occurred, it would-have presumably been accompanied by warmer
167 regional temperatures, but t independent paleoclimate records exist in the region which
168 show no such shift. Land-based glaciers in the Gulf of Alaska region underwent a period
169 of advance during the last half of the 19th century in Southern Alaska, thought to indicate
170 persistently cooler temperatures [Calkin et al., 2001; Wiles et al., 2004]. In addition, tree-
171 ring based reconstructions of January-September temperature across the entire Gulf of
172 Alaska region showed a significant cold shift in the 1840s [Wilson et al., 2007].
173 Furthermore, there is an apparent increasing trend in the Logan $\delta^{18}\text{O}$ since the mid 20th
174 century, which, under the controls identified here, would be consistent with the trend
175 towards a deeper wintertime AL observed over the same period [Bograd et al., 2002].

176 Our GCM analysis of circulation controls on the SW Yukon $\delta^{18}\text{O}$, when considered
177 alongside other paleoclimatic evidence, suggests that the observed shift in the middle of
178 the 19th century was associated with a weakening of the Aleutian Low and weakened
179 southerly moisture transport. An associated cooling in the Gulf of Alaska region would

180 contrast with the shift towards warmer conditions seen across much of the rest of the
181 Arctic [Smol et al., 2005], illustrating the importance of considering regional changes in
182 paleoclimatic reconstructions [Jones and Mann, 2003]. A similar phenomenon was found
183 in modeling the temperature difference between the late 17th and 18th centuries, when
184 emergence from the Maunder Minimum corresponded to a widespread winter-warming
185 across the Northern Hemisphere, with the exception of the Gulf of Alaska and North
186 Atlantic regions, which exhibited significant cooling [Shindell et al., 2001]. The Gulf of
187 Alaska, in particular, would appear to be a region where inter-decadal temperature
188 changes are frequently out of phase with those across the North American and Eurasian
189 land masses.

190 **Acknowledgements**

191 This work was supported by the Canadian Foundation for Climate and Atmospheric
192 Sciences through the Polar Climate Stability Network, and for RF by a graduate
193 scholarship from the Natural Sciences and Engineering Research Council of Canada. We
194 thank Allegra LeGrande and Sophie Lewis for assistance with the GCM.

195 **References**

- 196 Alley, R. B., and K. M. Cuffey, Oxygen- and Hydrogen-Isotopic Ratios of Water in
197 Precipitation: Beyond Paleothermometry, 527-553 pp., Reviews in Mineralogy and
198 Geochemistry, Mineralogical Soc. America, Washington DC, 2001.
- 199 Anderson, L., M. B. Abbott, B. P. Finney, and S. J. Burns, Regional Atmospheric
200 Circulation Change in the North Pacific During the Holocene Inferred From Lacustrine
201 Carbonate Oxygen Isotopes, Yukon Territory, Canada, *Quaternary Research*, 64(1), 21-
202 35, 2005.
- 203 Bograd, S., et al., On the changing seasonality over the North Pacific, *Geophys. Res.*
204 *Lett.*, 29(9), artn 1333, doi: 10.1029/2001gl013790, 2002.
- 205 Calkin, P. E., G. C. Wiles, and D. J. Barclay, Holocene coastal glaciation of Alaska,
206 *Quat. Sci. Rev.*, 20(1-3), 449-461, 2001.
- 207 Dansgaard, W. (1964), Stable Isotopes in Precipitation, *Tellus*, 16(4), 436-468.
- 208 D'Arrigo, R. et al., Tropical-North Pacific Climate Linkages Over the Past Four
209 Centuries, *J. of Clim.*, 18(24), 5253-5265, 2005.
- 210 Fisher, D. A. et al., Stable isotope records from Mount Logan, Eclipse ice cores and
211 nearby Jellybean Lake. Water cycle of the North Pacific over 2000 years and over five
212 vertical kilometres: sudden shifts and tropical connections, *Geographie physique et*
213 *Quaternaire*, 58(2-3), 337-352, 2004.
- 214 Holdsworth, G., H. R. Krouse, and M. Nosal, Ice core climate signals from Mount Logan,
215 Yukon, A.D. 1700-1897, in *Climate since A.D. 1500*, edited by R. S. Bradley and P. D.
216 Jones , pp. 483-504, Routledge, London, 1992.
- 217 IAEA (2001), GNIP Maps and animations, International Atomic Energy Agency,
218 Vienna. <http://isohis.iaea.org>.
219
- 220 Jones, P. D. and M. E. Mann, Climate Over Past Millennia, *Rev. of Geophys.*, 42(2),
221 2004.
- 222 Joussaume, S., et al. (1984), A General-Circulation Model of Water Isotope Cycles in the
223 Atmosphere, *Nature*, 311(5981), 24-29.
224
- 225 Mock, C. J., P. J. Bartlein, and P. M. Anderson, Atmospheric circulation patterns and
226 spatial climatic variations in Beringia, *Int. J. Clim.*, 18(10), 1085-1104, 1998.
- 227 Moore, G. W. K., G. Holdsworth, and K. Alverson, Climate Change in the North Pacific
228 Region Over the Past Three Centuries, *Nature*, 420(6914), 401-403, 2002.
- 229 Peixoto, J. P. and Oort, A. H. Physics of Climate. 520pp. 1992. New York, NY., AIP
230 Press.

- 231 Rayner, N. A., et al. , Global analyses of sea surface temperature, sea ice, and night
 232 marine air temperature since the late nineteenth century, *J. Geophys. Res., [Atmos.]*,
 233 *108(D14)*, 2003.
- 234 Rogers, J. C., J. F. Bolzan, and V. A. Pohjola, Atmospheric Circulation Variability
 235 Associated With Shallow-Core Seasonal Isotopic Extremes Near Summit, Greenland, *J.*
 236 *Geophys. Res., [Atmos.]*, *103(D10)*, 11205-11219, 1998.
- 237 Rupper, S., E. J. Steig, and G. Roe, The Relationship Between Snow Accumulation at
 238 Mt. Logan, Yukon, Canada, and Climate Variability in the North Pacific, *J. Clim.*,
 239 *17(24)*, 4724-4739, 2004.
- 240 Schmidt, G. A., G. Hoffmann, D. T. Shindell, and Y. Y. Hu, Modeling Atmospheric
 241 Stable Water Isotopes and the Potential for Constraining Cloud Processes and
 242 Stratosphere-Troposphere Water Exchange, *J. Geophys. Res., [Atmos.]*, *110(D21)*, 2005.
- 243 Shindell, D. T., G. A. Schmidt, M. E. Mann, D. Rind, and A. Waple, Solar Forcing of
 244 Regional Climate Change During the Maunder Minimum, *Science*, *294(5549)*, 2149-
 245 2152, 2001.
- 246 Smol, J. P. et al., Climate-Driven Regime Shifts in the Biological Communities of Arctic
 247 Lakes, *Proc. Natl. Acad. Sci. U. S. A.*, *102(12)*, 4397-4402, 2005.
- 248 Trenberth, K. E. and J. W. Hurrell, Decadal Atmosphere-Ocean Variations in the Pacific,
 249 *Clim. Dyn.*, *9(6)*, 303-319, 1994.
- 250 Trenberth, K. E., et al., Progress During Toga in Understanding and Modeling Global
 251 Teleconnections Associated With Tropical Sea Surface Temperatures, *J. Geophys. Res.*,
 252 *[Oceans]*, *103(C7)*, 14291-14324, 1998.
- 253 Vuille, M., R. S. Bradley, M. Werner, R. Healy, and F. Keimig, Modeling Delta O-18 in
 254 Precipitation Over the Tropical Americas: 1. Interannual Variability and Climatic
 255 Controls, *J. Geophys. Res., [Atmos.]*, *108(D6)*, 2003.
- 256 Wallace, J. M., and D. S. Gutzler (1981), Teleconnections in the Geopotential Height
 257 Field During the Northern Hemisphere Winter, *Mon. Weather Rev.*, *109(4)*, 784-812.
 258
- 259 Werner, M. and M. Heimann, Modeling Interannual Variability of Water Isotopes in
 260 Greenland and Antarctica, *J. Geophys. Res., [Atmos.]*, *107(D1-D2)*, 2002.
- 261 Wiles, G. C., R. D. D'Arrigo, R. Villalba, P. E. Calkin, and D. J. Barclay, Century-scale
 262 solar variability and Alaskan temperature change over the past millennium, *Geophys.*
 263 *Res. Lett.*, *31(15)* , 2004.
- 264 Wilson, R., G. Wiles, R. D'Arrigo, and C. Zweck, Cycles and shifts: 1,300 years of
 265 multi-decadal temperature variability in the Gulf of Alaska, *Clim. Dyn.*, *28(4)*, 425-440,
 266 2007.

267 Zhu, X. J., J. L. K. Sun, Z. Y. Liu, Q. Y. Liu, and J. E. Martin, A Synoptic Analysis of
268 the Interannual Variability of Winter Cyclone Activity in the Aleutian Low Region, *J. of*
269 *Clim.*, 20(8), 1523-1538, 2007.

270 **List of figures**

271 Figure 1. The Mt. Logan Northwest Col annual $\delta^{18}\text{O}$ record from Holdsworth et al.
272 [1992].

273
274 Figure 2. Annual circulation and moisture-flux correlation maps for: a) precipitation $\delta^{18}\text{O}$
275 b) mid-tropospheric vapor $\delta^{18}\text{O}$ c) precipitation amount and d) surface temperature over
276 the SW Yukon, bounded by the black box. The colored shading indicates the correlation
277 between the climate parameter over the SW Yukon and SLP (panels a, c, d) and
278 geopotential height at 630hPa (panel b). Vector lengths indicate the correlation between
279 the climate parameters over the SW Yukon and moisture flux in each of the u and v
280 direction, for surface (panels a, c, d) and mid-tropospheric (panel b) moisture flux. For
281 all meteorological fields, only correlations significant at a 95% level are shown.

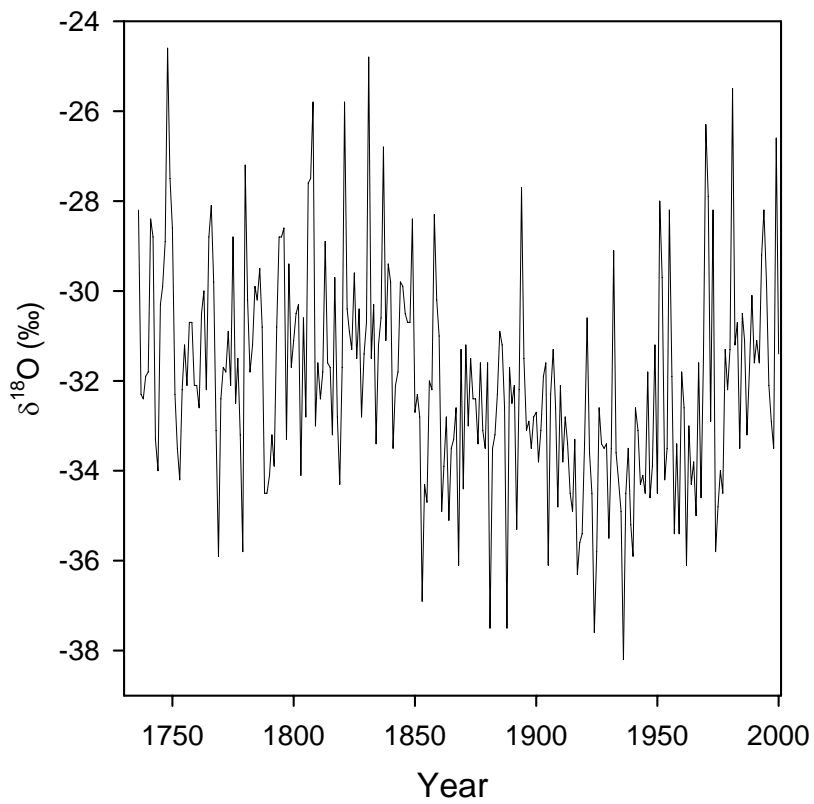
282
283 Figure 3. Same as Figure 2, but for cool-season (September to February).
284

285 **Tables**

286 **Table 1. Precipitation $\delta^{18}\text{O}$ (‰) observed at GNIP stations and modeled under GISS.**

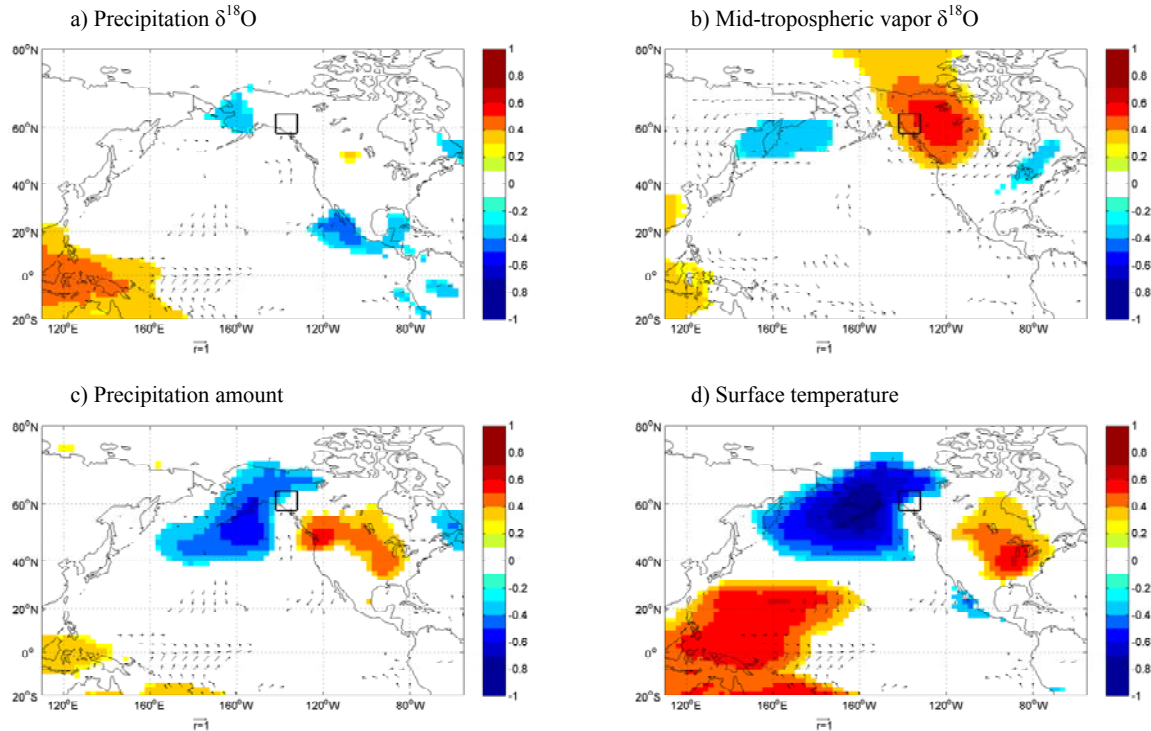
Location	Lat	Lon	GNIP		GISS	
			DJF	JJA	DJF	JJA
Barrow, AK	71°17N	156°45W	-21.1	-14.7	-22.7	-15.8
Bethel, AK	60°47N	161°45W	-15.1	-11.0	-15.7	-12.1
Whitehorse, YK	60°43N	135°03W	-23.8	-18.7	-18.3	-18.2
Yellowknife, NWT	62°27N	114°24W	-25.1	-16.8	-24.2	-14.9

287 **Figures**



288

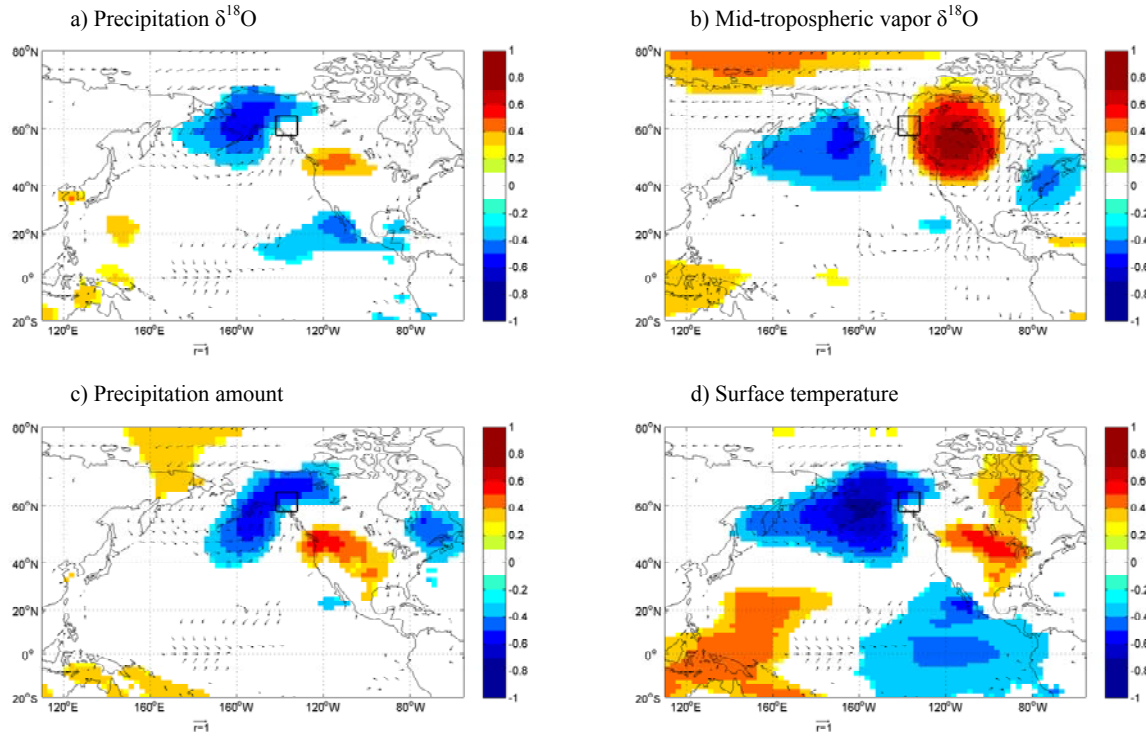
289 **Figure 1. The Mt. Logan Northwest Col annual $\delta^{18}\text{O}$ record from Holdsworth et al. [1992].**



290

291 **Figure 2. Annual circulation and moisture-flux correlation maps for: a) precipitation $\delta^{18}\text{O}$ b) mid-**
 292 **tropospheric vapor $\delta^{18}\text{O}$ c) precipitation amount and d) surface temperature over the SW Yukon,**
 293 **bounded by the black box. The colored shading indicates the correlation between the climate**
 294 **parameter over the SW Yukon and SLP (panels a, c, d) and geopotential height at 630hPa (panel b).**
 295 **Vector lengths indicate the correlation between the climate parameters over the SW Yukon and**
 296 **moisture flux in each of the u and v direction, for surface (panels a, c, d) and mid-tropospheric**
 297 **(panel b) moisture flux. For all meteorological fields, only correlations significant at a 95% level are**
 298 **shown.**

299



300

301 **Figure 3. Same as Figure 2, but for cool-season (September to February).**

302